

Rate-Dependent Interaction between Thin Films and Interface during Micro/Nanoscale Transfer Printing

Dongjie Jiang^a, Xue Feng^{a}, Binrui Qu^a, Yong Wang^b, Daining Fang^{c*}*

^aAML, Department of Engineering Mechanics, Tsinghua University, Beijing 100084, China

^bDepartment of Mechanics, Zhejiang University, Hangzhou, 310027, China

^cLTCS and College of Engineering, Peking University, Beijing, 100871, China

* Corresponding author, Email: fengxue@tsinghua.edu.cn, fangdn@pku.edu.cn

Supporting Text A: Principle of Cohesive Elements

Cohesive element modeling is based on the continuum framework. Rahul Kumar et al. elaborated the establishment of cohesive elements in finite element modeling.¹⁶ The weak form of momentum equations accounting for cohesive zone is given as

$$\int_V \boldsymbol{\sigma} : \delta \mathbf{d} \, dV + \int_S \mathbf{T} \cdot \delta \dot{\boldsymbol{\Delta}} \frac{1}{J} \, dS - \int_A \mathbf{F} \cdot \delta \mathbf{v} \, dA = 0 \quad (\text{S1})$$

where $\boldsymbol{\sigma}$ is the Cauchy stress tensor; $\delta \mathbf{d}$ is the virtual deformation rate tensor; \mathbf{T} is the vector of cohesive tractions; $\boldsymbol{\Delta}$ is the vector of interfacial separation displacement; \mathbf{F} is the vector of externally applied tractions; $\delta \mathbf{v}$ is the vector of the virtual velocity field; V is the current volume of the material; S is the current internal surface area over which the cohesive tractions are acting; J is the Jacobian of the transformation between the current configuration and reference configuration of the cohesive surfaces; A is the current external surface area over which the external tractions are applied.

An implicit finite element solution based on Newton-Raphson iterations requires the tangent stiffness matrix of each element. The implementation of cohesive elements then leads to the evaluation of the first variation for the second term of Eq. S1. This virtual work rate of the cohesive tractions is given as

$$\delta W_c = \int_S (T_n \cdot \delta \dot{\Delta}_n + T_t \cdot \delta \dot{\Delta}_t) \frac{1}{J} \, dS \quad (\text{S2})$$

where T_n and T_t are the normal and tangential tractions respectively, and $\delta \dot{\Delta}_n$ and $\delta \dot{\Delta}_t$ are the virtual normal and tangential interfacial separation velocities. Substituting the virtual interfacial separation velocities in terms of the cohesive element nodal shape functions and the nodal virtual interfacial separation velocities, the discretized virtual work rate in the current configuration, $\delta \bar{W}_c$, is obtained as

$$\delta \bar{W}_c = \int_S (\delta \dot{\Delta}_n^T \mathbf{N}^T T_n + \delta \dot{\Delta}_t^T \mathbf{N}^T T_t) \frac{1}{J} \, dS \quad (\text{S3})$$

where the bar denotes cohesive element nodal values, the superscript T denotes a transpose operation, and \mathbf{N} is the vector of cohesive element nodal shape functions. The form of eq S3 ensures that the

virtual work can be used with finite elements that are formulated using an upgraded Lagrangian formulation. The first variation of the virtual work, $d\delta\bar{W}_c$ can be obtained as

$$d\delta\bar{W}_c = \int_S \left(\delta\dot{\Delta}_n^T \mathbf{N}^T dT_n + \delta\dot{\Delta}_t^T \mathbf{N}^T dT_t \right) \frac{1}{J} dS + \int_S \left(\delta\dot{\Delta}_n^T \mathbf{N}^T T_n + \delta\dot{\Delta}_t^T \mathbf{N}^T T_t \right) d \left(\frac{1}{J} \right) dS \quad (\text{S4})$$

where dT_n and dT_t are the increments of normal and tangential tractions, respectively. In eq S4, the second term accounts for the stretching of the cohesive element. For small stretching of the cohesive element this term is negligible and the first variation of the virtual work can be approximated as

$$d\delta\bar{W}_c \approx \int_S \left(\delta\dot{\Delta}_n^T \mathbf{N}^T dT_n + \delta\dot{\Delta}_t^T \mathbf{N}^T dT_t \right) \frac{1}{J} dS \quad (\text{S5})$$

Multiplying cohesive material Jacobian matrix $[\mathbf{D}]$ and incremental interfacial separation displacements gives increments of tractions as

$$\begin{Bmatrix} dT_n \\ dT_t \end{Bmatrix} = [\mathbf{D}] \begin{Bmatrix} d\Delta_n \\ d\Delta_t \end{Bmatrix} \quad (\text{S6})$$

where $[\mathbf{D}]$ is defined as

$$[\mathbf{D}] = \begin{bmatrix} \frac{\partial T_n}{\partial \Delta_n} & \frac{\partial T_n}{\partial \Delta_t} \\ \frac{\partial T_t}{\partial \Delta_n} & \frac{\partial T_t}{\partial \Delta_t} \end{bmatrix} \quad (\text{S7})$$

Substituting the increments of tractions in terms of the incremental interfacial separation velocities from eq S7 into eq S6, and writing the incremental interfacial separation velocities in terms of the incremental cohesive element nodal velocities, the tangent stiffness matrix takes the form

$$\mathbf{K}_T = \int_S [\mathbf{B}]^T [\mathbf{D}] [\mathbf{B}] \frac{1}{J} dS \quad (\text{S8})$$

where $[\mathbf{B}]$ is the matrix of cohesive element nodal shape functions that relates the nodal velocities to the velocities of the interfacial separation displacement field within the cohesive element. The stiffness matrix implemented using eq S8 gives an approximate tangent for Newton-Raphson iterations.

Supporting Text B: Cohesive Law

Mechanical behavior of the cohesive zone can be represented by a phenomenological bilinear cohesive law given as following

For $\tilde{\Delta}_n > 0$,

$$T_n = \begin{cases} \frac{\tilde{\Delta}_n}{\tilde{\Delta}_{\max}} \sigma_{\max}, (\tilde{\Delta} \leq \tilde{\Delta}_{\max}) \\ \frac{\tilde{\Delta}_n}{\tilde{\Delta}} \frac{1 - \tilde{\Delta}}{1 - \tilde{\Delta}_{\max}} \sigma_{\max}, (\tilde{\Delta} > \tilde{\Delta}_{\max}) \end{cases} \quad (\text{S9})$$

$$T_t = \begin{cases} \frac{\tilde{\Delta}_t}{\tilde{\Delta}_{\max}} \frac{\Delta_n^c}{\Delta_t^c} \sigma_{\max}, (\tilde{\Delta} \leq \tilde{\Delta}_{\max}) \\ \frac{\tilde{\Delta}_t}{\tilde{\Delta}} \frac{1 - \tilde{\Delta}}{1 - \tilde{\Delta}_{\max}} \frac{\Delta_n^c}{\Delta_t^c} \sigma_{\max}, (\tilde{\Delta} > \tilde{\Delta}_{\max}) \end{cases} \quad (\text{S10})$$

For $\tilde{\Delta}_n = 0$,

$$T_t = \begin{cases} \frac{\tilde{\Delta}_t}{\tilde{\Delta}_{\max}} \frac{\Delta_n^c}{\Delta_t^c} \sigma_{\max}, (\tilde{\Delta} \leq \tilde{\Delta}_{\max}) \\ \frac{\tilde{\Delta}_t}{\tilde{\Delta}} \frac{1 - \tilde{\Delta}}{1 - \tilde{\Delta}_{\max}} \frac{\Delta_n^c}{\Delta_t^c} \sigma_{\max}, (\tilde{\Delta} > \tilde{\Delta}_{\max}) \end{cases} \quad (\text{S11})$$

where σ_{\max} and τ_{\max} are the interface normal strength and tangential strength, respectively; Δ_n^c and Δ_t^c are the critical normal and tangential interfacial separations when complete separation occurs; $\tilde{\Delta}_n$, $\tilde{\Delta}_t$ and $\tilde{\Delta}$ are the nondimensionalized normal, tangential and total displacement jumps, respectively, and defined as:

$$\tilde{\Delta}_n = \frac{\Delta_n}{\Delta_n^c}, \tilde{\Delta}_t = \frac{\Delta_t}{\Delta_t^c}, \tilde{\Delta} = \sqrt{\tilde{\Delta}_n^2 + \tilde{\Delta}_t^2} \quad (\text{S12})$$

$\tilde{\Delta}_{\max}$ is the corresponding value of $\tilde{\Delta}_n$ or $\tilde{\Delta}_t$ when the interface normal strength or tangential strength reaches its peak value.

For pure opening ($\Delta_t = 0$) and pure shearing separation ($\Delta_n = 0$), the normal and tangential tractions versus separation are graphically depicted in Figure S1 and Figure S2, respectively. The normal fracture energy ϕ_n and the tangential fracture energy ϕ_t , can be written in terms of cohesive normal strength σ_{\max} and tangential strength τ_{\max} as

$$\phi_n = \frac{1}{2} \sigma_{\max} \Delta_n^c, \phi_t = \frac{1}{2} \tau_{\max} \Delta_t^c \quad (\text{S13})$$

The ϕ_n and ϕ_t means the work that need to be done to separate the interface per unit area under pure normal and tangential separations, respectively.

In this paper, we take the interfacial toughness Γ_0 and critical interfacial separation displacement δ_{cr} as

$$\Gamma_0 = \phi_n = \phi_t \quad (\text{S14})$$

$$\delta_{cr} = \Delta_n^c = \Delta_t^c \quad (\text{S15})$$

Figure Captions

Figure S1. The normal cohesive traction versus separation for pure opening separation

Figure S2. The tangential cohesive traction versus separation for pure shearing separation

Figure S1.

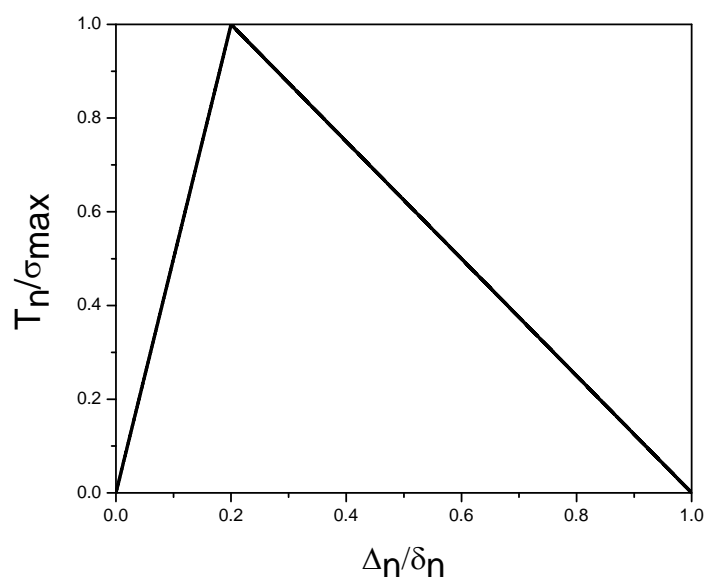


Figure S2.

